Kashf Journal of Multidisciplinary Research
Vol: 02 - Issue 4 (2025)
P-ISSN: 3007-1992 E-ISSN: 3007-200X
https://kjmr.com.pk

PROPAGATION OF ELECTROMAGNETIC SURFACE WAVES AT CHIRAL LOADED MAGNETIZED PLASMA PLANAR STRUCTURE

M. Arif
Department of Physics, University of Agriculture, Faisalabad, Pakistan.

M. Umair
Department of Physics, University of Agriculture, Faisalabad, Pakistan.

A. Ghaffar
Department of Physics, University of Agriculture, Faisalabad, Pakistan.

Muhammad Zeshan Yaqoob*
Department of Physics, Government College University, Faisalabad, Pakistan.

****Corresponding author: Muhammad Zeshan Yaqoob (**zeeshaan32@yahoo.com**)***

Article Info

Abstract

Chiral media, which are found in both natural and synthetic metamaterials, possess unique and remarkable optical characteristics that arise from their inherent structural asymmetry. The behavior of electromagnetic surface waves (EMSWs) at the chiral and magnetized plasma interface are theoretically analyzed. The numerical results are obtained to examine the impact of chirality and plasma characteristics on hybrid EMSWs in the terahertz (THz) frequency region. Results suggest that chirality and magnetized plasma parameters (plasma frequency and cyclotron frequency) have a pivotal role in the modeling and precise tuning of the EMSWs. It is found that higher chirality result in an increased effective mode index, which can be reduced by raising the plasma frequency and cyclotron frequency. The numerical results demonstrate a strong dependence of the effective mode index on the operating frequency. Therefore, the characteristics of EMSWs can be tuned by controlling the above mentioned parameters. It is demonstrated that EMSWs at the proposed model exhibit unique characteristics as compared to conventional EMSWs at a dielectric-metal interface. Moreover, to verify the authenticity of the EMSW traits, the field profiles for the chiral medium are also presented. This work holds promising potential for fascinating applications in the nanophotonic community, particularly in the development of high-density nanophotonic chips and advanced chiral sensing systems operating in the THz frequency range.

Keywords:

Electromagnetic surface wave, Chiral, Magnetized plasma, Characteristic equation, Dispersion relation, Terahertz.

Introduction

Over the past few decades, electromagnetic surface waves (EMSWs) have gained importance in the field of optics [1-3]. EMSWs can exist at the interface of dissimilar media for any planar or curvilinear planar structure, and they exponentially decay while propagating. Surface enhanced spectroscopy is one of the most exciting areas of research where EMSWs have made a significant impact in this field. The use of EMSWs in improving photovoltaic solar cells' ability to absorb light has attracted a lot of attention. Several methods are used to enhance light harvesting efficiency through the utilization of EMSWs. In optical technology, EMSWs exhibit a broad spectrum of potential applications, particularly in communication technology. Their integration into fiber optics has the potential to substantially improve both short-range and long-range signals in communication and reduce dissipation [4, 5].

A chiral material is defined as a macroscopically continuous medium consisting of uniformly distributed and randomly oriented equivalent chiral objects. The purely geometric concept known as "chirality" or "handedness" is described by the lack of bilateral symmetry of an object with its mirror image [6]. If a linearly polarized wave is incident normally on a chiral material, it splits into two orthogonal modes with different phase velocity, namely the right circularly polarized and left circularly polarized modes. As the two modes emerge from the chiral material, they recombine once again to generate a wave that is linearly polarized, and its plane of polarization is rotated relative to that of the incident electromagnetic wave [7]. The significant features of the chiral materials are the optical activity, which has the ability to rotate the polarization plane of a wave passing through it, and their circular dichroism, which is the differential absorption of a LCP or RCP wave [8]. Due to the presence of two distinct Eigen modes in chiral material, birefringence occurs at the interface of the chiral and achiral material. Isotropic birefringent materials, known as chiral materials, exhibit both electric and magnetic polarizations in response to electric or magnetic excitation [9]. In a typical dielectric material, the magnetic field **B** is only dependent on the magnetic induction **H**, and the displacement vector **D** is alone dependent on the electric field **E**. However, in a chiral material, **D** and **B** depend on a combination of the both **E** and **H**. Therefore, in-depth mathematical modeling is necessary to comprehend the characteristics of chiral materials, and constitutive relations for ordinary dielectrics are modified for this purpose. Chiral materials feature a magneto-electric coupling that produces the intriguing electromagnetic field properties, in contrast to ordinary materials are characterized by electric permittivity and magnetic permeability. In recent past, chiral materials have attracted huge attention due to their numerous innovative applications and the feasibility of fabricating these novel materials for microwave and millimeter-wave regimes. Recently, a number of fundamental problems related to the interaction of electromagnetic waves with chiral materials have been investigated and reported in the literature [10-13].

Plasmas used in plasma metamaterials and plasma photonic crystals have attracted considerable interest because of their dynamic tunable properties, which offer some unique and notable advantages. Since plasmas have some exceptional features in comparison to ordinary materials as well as prominent applications, we have good reason to believe that the synthetic composites that involve or substitute plasmas can have exceptional properties that lead to many fascinating phenomena. The permittivity tunability and the calibration of its amplitude on the complex coordinate plane can be controlled by the input power supply used for creating the plasma and adjusting its pressure and temperature [14]. Since the plasma can help us to realize tunable EMSWs, a discussion of their applications in the field of EMSWs is warranted. Magnetized plasma has optical anisotropy [15-18], which leads to lucrative and marvelous properties such as the coexistence of transverse magnetic and transverse electric surface wave modes. One notable advantage of this optical anisotropy is the increase in propagation length [19]. In modern applications, external applied magnetic field can be used to control the transmission, reflection, and absorption of waves, which enables us to tune them as desired. Laroussi and Roth examined numerical results to explore how the potential applications of the ambient magnetic field offer advantages in wave absorption around the cyclotron frequency [20]. They discovered that while the absorption of waves around the cyclotron frequency is amplified by the magnetic field, but it decreases as the external magnetic field increases. While Petrin [21] found an increase in transmission compared to isotropic plasma. Numerous studies have examined the electromagnetic waves in plasma medium for various applications, including industrial plasma and plasma radar absorbers [22-25]. Plasma medium opens a new avenue for the fabrication of microwave photonic and nano-photonic devices. Majedi et al.

studied the propagation of the EMSWs in a semi bounded quantum plasma with ½ spin magnetization under collisional conditions [26]. Considering the effective dielectric function of the anisotropic plasma, Qi et al. analyzed the surface plasmon polaritons that were excited at the dielectric and a magnetized plasma interface. More recently, Zhu et al. explored the characteristics of graphene surface plasmons at the interface of a graphene sheet and magnetic plasma using a quantum hydrodynamic model [27]. These studies suggest that it is important and meaningful to study EMSWs in magnetized plasma. It has been understood that unidirectional surface waves can emerge at the interface of a gyrotropic medium and any isotropic material under suitable conditions and in desired frequency ranges. Interest in this subject has recently increased, and the potential for achieving completely unidirectional electromagnetic wave propagation along with a considerable degree of field localization and confinement is particularly fascinating. In contrast to unmagnetized plasma, magnetized plasma has anisotropy, dispersion, and dissipation simultaneously, which are novel and important characteristics to the study of EMSWs. Magnetized plasma has an extra degree of freedom due to the applied external magnetic field. The new and fascinating aspect of this work is the derivation of analytical formulas for the dispersion relation from the dielectric parameter of the magnetized plasma. The significant uses of EMSWs in the THz regime inspired us to propose a chiral–magnetized plasma waveguide structure that has not yet been presented.

Methodology

An electromagnetic wave with harmonic time dependence $e^{i\omega t}$ and longitudinal propagation constant β is excited at the interface of a chiral material and magnetized plasma. It propagates along the z-axis and attenuates exponentially along the x-axis. The upper region, $x > 0$, is a chiral material, and lower region i.e. $x < 0$, is magnetized plasma, as depicted in Figure 1.

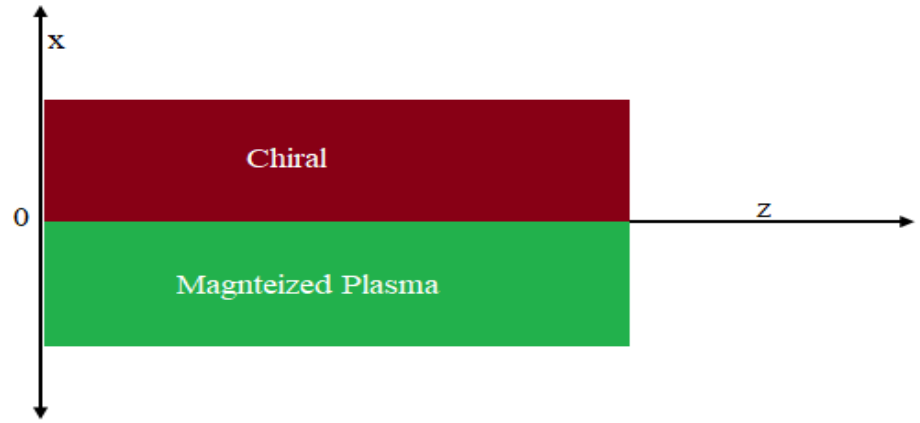

Figure 1: Geometrical representation of chiral–magnetized plasma planar interface.

The magnetized plasma can be defined with the help of following constitutive relations.

$$\mathbf{D} = \varepsilon_0 \bar{\bar{\boldsymbol{\varepsilon}}}.\mathbf{E} \tag{1}$$

$$\mathbf{H} = 1/\mu\mathbf{B} \tag{2}$$

Here μ and $\bar{\bar{\boldsymbol{\varepsilon}}}$ are permeability and permittivity of the material and the tensor $\bar{\bar{\boldsymbol{\varepsilon}}}$ is defined as

$$\bar{\bar{\varepsilon}} = \begin{vmatrix} \varepsilon_1 & -\varepsilon_2 i & 0 \\ i\varepsilon_2 & \varepsilon_1 & 0 \\ 0 & 0 & \varepsilon_3 \end{vmatrix} \tag{3}$$

where

$$\varepsilon_1 = \varepsilon_0 \left(1 - \frac{\omega_p^2}{\omega^2 - \omega_p^2}\right) \quad (4)$$

$$\varepsilon_2 = \varepsilon_0 \left[\frac{\omega_w * \omega_p^2}{\omega * (\omega^2 - \omega_w^2)}\right] \quad (5)$$

$$\varepsilon_3 = \varepsilon_0 \left(1 - \frac{\omega_p^2}{\omega^2}\right) \quad (6)$$

$$\omega_p = \sqrt{\frac{n * e^2}{m * \epsilon_0}} \quad (7)$$

$$\Omega_c = \frac{e * B}{m} \quad (8)$$

The mutually coupled wave equations E_z and H_z in the magnetized plasma given below are obtained by using Maxwell's equations.

$$\begin{bmatrix} \nabla_t^2 E_z \\ \nabla_t^2 H_z \end{bmatrix} + \begin{bmatrix} T_{11} & jT_{12} \\ jT_{13} & T_{14} \end{bmatrix} \begin{bmatrix} E_z \\ H_z \end{bmatrix} = 0 \quad (9)$$

where

$$T_{11} = \frac{(-\beta^2 + \omega^2 \mu_0 \rho_1)\rho_3}{\rho_1} \quad (10)$$

$$T_{12} = \frac{\omega_p \mu \beta \rho_2}{\rho_1} \quad (11)$$

$$T_{13} = -\frac{\beta \omega \rho_2 \rho_3}{\epsilon_1} \quad (12)$$

$$T_{14} = \frac{\omega^2 \mu (\rho_1^2 - \rho_2^2)}{\rho_1} - \beta^2 \quad (13)$$

$$q_{\pm 2} = \frac{1}{2}\{T_{11} + T_{14} \pm \sqrt{(T_{11} + T_{14})^2 - 4(T_{11} T_{14} - T_{13} T_{12})}\}. \quad (14)$$

The hybrid nature of the propagating modes is defined by corresponding Eigen-functions as

$$(E_z, H_z) = (E_z, i\alpha_{\pm} E_z) \quad (15)$$

Where the mode hybrid factor is $\alpha_{\pm} = \frac{1}{T_{12}}(T_{11} - q_{\pm}^2)$.

The field equations in the direction of the propagation of EMSWs are given as

$$\left.\begin{aligned} E_z &= [U_1 e^{-q_+ x} + U_2 e^{-q_- x}] e^{-i\beta z} \\ H_z &= i\,[U_1 \alpha_+ e^{-q_+ x} + U_2 \alpha_- e^{-q_- x}] e^{-i\beta z} \end{aligned}\right\} \quad (16)$$

The remaining field components for the plasma medium are obtained from [21]. The constitutive relationship for the chiral material is given as

$$D = \varepsilon_c E - i\xi_c \sqrt{\mu_0 \varepsilon_0}\, H \quad (17)$$

$$B = \mu_c H + i\xi_c \sqrt{\mu_0 \varepsilon_0}\, E. \quad (18)$$

The field components for the chiral material are

$$H_y = \frac{-\frac{\alpha_1}{k_+} U_3 e^{-\alpha_1 x} + \frac{\alpha_2}{k_-} U_4 e^{-\alpha_2 x}}{2i\eta} \quad (19)$$

$$H_z = \frac{e^{-\alpha_1 x} U_3 - U_4 e^{-\alpha_2 x}}{2i\eta} \quad (20)$$

$$E_z = \frac{e^{-\alpha_1 x} U_3 + U_4 e^{-\alpha_2 x}}{2} \quad (21)$$

$$E_y = \frac{-\frac{\alpha_1}{k_+} U_3 e^{-\alpha_1 x} + \frac{\alpha_2}{k_-} U_4 e^{-\alpha_2 x}}{2} \quad (22)$$

$$k_\pm = (s\sqrt{\mu_c \varepsilon_c / \mu_0 \varepsilon_0} \pm k)\omega/c. \quad (23)$$

$s = +1$ and $s = -1$ are the wave numbers for the RCP and LCP polarized electromagnetic waves, respectively, as reported in [28].

At the interface, the following boundary conditions are applied:

$$\hat{x} \times [H_1 - H_2] = 0 \quad (24)$$

$$\hat{x} \times [E_1 - E_2] = 0. \quad (25)$$

By applying above equations (boundary conditions) at the interface of the chiral–magnetized plasma yield the following characteristics equation:

$$\begin{bmatrix} b_{11} & b_{12} & b_{13} & b_{14} & U_1 \\ b_{21} & b_{22} & b_{23} & b_{24} & U_2 \\ b_{31} & b_{32} & b_{33} & b_{34} & U_3 \\ b_{41} & b_{42} & b_{43} & b_{44} & U_4 \end{bmatrix} = 0 \quad (26)$$

The above equation set yields the characteristics equation given below.

$$\begin{vmatrix} b_{11} & b_{12} & b_{13} & b_{14} \\ b_{21} & b_{22} & b_{23} & b_{24} \\ b_{31} & b_{32} & b_{33} & b_{34} \\ b_{41} & b_{42} & b_{43} & b_{44} \end{vmatrix} = 0 \quad (27)$$

where

$b_{11} = \frac{\alpha_1}{k_+}$, $b_{12} = \frac{\alpha_2}{k_-}$, $b_{13} = \eta q_+ (f + b\alpha_+)$, $b_{14} = \eta q_- (f + b\alpha_-)$, $b_{21} = -\frac{\alpha_1}{k_+}$, $b_{22} = \frac{\alpha_2}{k_-}$, $b_{23} = q_+(b - d\alpha_+)$, $b_{24} = q_-(b - d\alpha_-)$, $b_{31} = 1$, $b_{32} = 1$, $b_{33} = -1$, $b_{34} = -1$, $b_{41} = 1$, $b_{42} = -1$, $b_{43} = -\eta\alpha_+$ and $b_{44} = \eta\alpha_-$.

Typically, only numerical methods can be employed to solve implicit transcendental equations like Equation (27).

Results and Discussion

The analytical results of the suggested model are reported in this section to analyze and understand the behavior of EMSW propagation at the chiral–magnetized plasma structure. The characteristic equation is derived from the analytical solution of the electromagnetic field components of given materials. Wolfram Mathematica software is used for computation and analysis of effective mode index. Where the effective mode index is defined as $Re(\frac{\beta}{k_0})$, where

β and k_0 are the propagation constant and wave number in free space, respectively.

The dispersive and resonance permittivity of a chiral medium are $\varepsilon_c = (1 - \frac{\omega_e^2}{\omega^2 - \omega^2 + i\omega\gamma_e})\varepsilon_0$ and $\kappa = \frac{\omega_k}{\omega^2 - \omega_{kR}^2 + i\omega\gamma_k}$, where $\gamma_k = \gamma_e = 0.05\omega_e$ and $\omega_k = \omega_e$ is the chirality strength, as presented in [28]. To determine the confinement of EMSWs for the proposed design, the effect of different parameters of plasma and chiral material i.e. plasma frequency, cyclotron frequency, and chirality on the effective mode index with respect to the operating frequency in the THz regime was analyzed. Figure 2 shows impact on the effective mode index with respect to the operating frequency under different plasma frequencies (i.e., $\omega_p = 1 * 10^8\ Hz, \omega_p = 2 * 10^8\ Hz, \omega_p = 3 * 10^8\ Hz,$ and $\omega_p = 4 * 10^8\ Hz$). The plasma frequency is defined as $\omega_p = \sqrt{\frac{n * e^2}{m s_0}}$, where n is density of electrons, e and m are the charge and mass of

electrons, ε_0 is the permittivity of free space. By increasing the plasma frequency, both the propagation bandgap and the effective mode index decreased. This phenomena reflects the higher confinement of EMSWs at the lower plasma frequency. The operating frequency of EMSWs under consideration ranges from 0 to 2.5 THz. It is also observed that an increase in the plasma frequency moves the dispersion curve to a high-frequency regime that reflects the lower confinement of the hybrid surface wave for the proposed design.

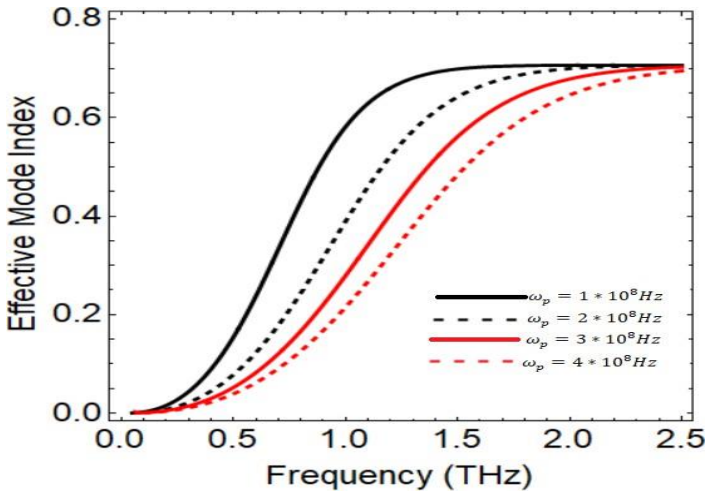

Figure 2: Influence of plasma frequency on effective mode index with respect to operating frequency.

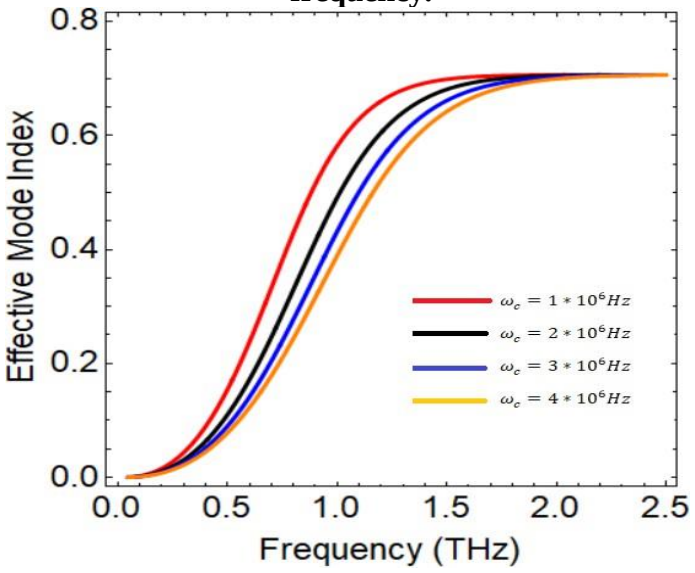

Figure 3: Influence of cyclotron frequency on effective mode index with respect to operating frequency.

Therefore high value of effective mode index may be achieved by decreasing the plasma frequency as reported in [29]. Figure 3 depicts the effects of the cyclotron frequency on the effective mode index with respect to the operating frequency of EMSWs. The cyclotron frequencies vary in the range of $\omega_c = 1 * 10^6 - 4 * 10^6\ Hz$. The cyclotron frequency is calculated as $\omega_c = \frac{eB}{m}$, where m, e, and B are the mass of electrons, charge of electrons, and

external magnetic field, respectively. The charge and mass of electrons are fixed, but the external applied magnetic field can be tuned. It is evident that, as the cyclotron frequency increases, the effective mode index decreases and the propagation bandgap starts squeezing. The characteristic peaks also move toward the higher frequency region. Figure 4 describes the impact of chirality on the effective mode index with respect to the operating surface wave frequency. The frequency band have range from 0 to 2.5 THz, while chirality increases from $\omega_k = 0.02\ \omega_e$ to $\omega_k = 0.08\ \omega_e$. With the increase in chirality parameter, the propagation bandgap starts squeezing, and the characteristics peaks shift towards the lower operating surface wave frequency region. It should be mentioned that a higher effective mode index can be obtained at a higher values of chirality. Figure 5 presents the fields profile for the chiral medium to verify the electromagnetic surface wave traits. The surface wave has two traits: it propagates at the interface of two dissimilar materials, and it decays exponentially as EMSWs propagate away from the interface. The red and blue dashed characteristic peaks show attenuation as it propagates away from the interface hence verifying the both conditions of EMSWs.

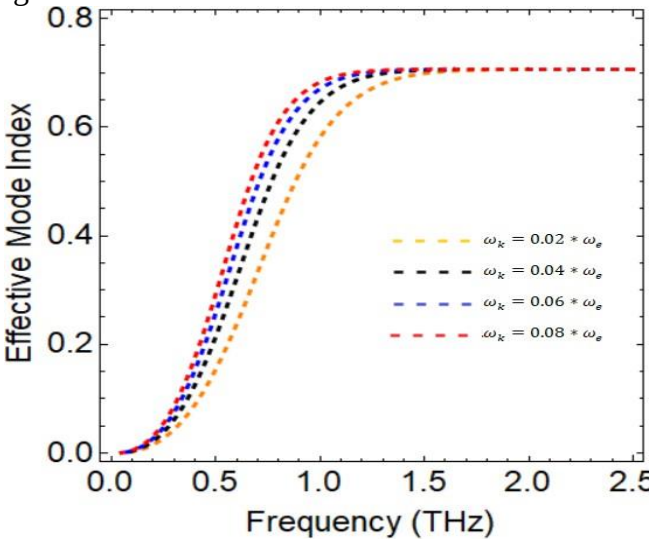

Figure 4: Influence of chirality on effective mode with respect to operating frequency.

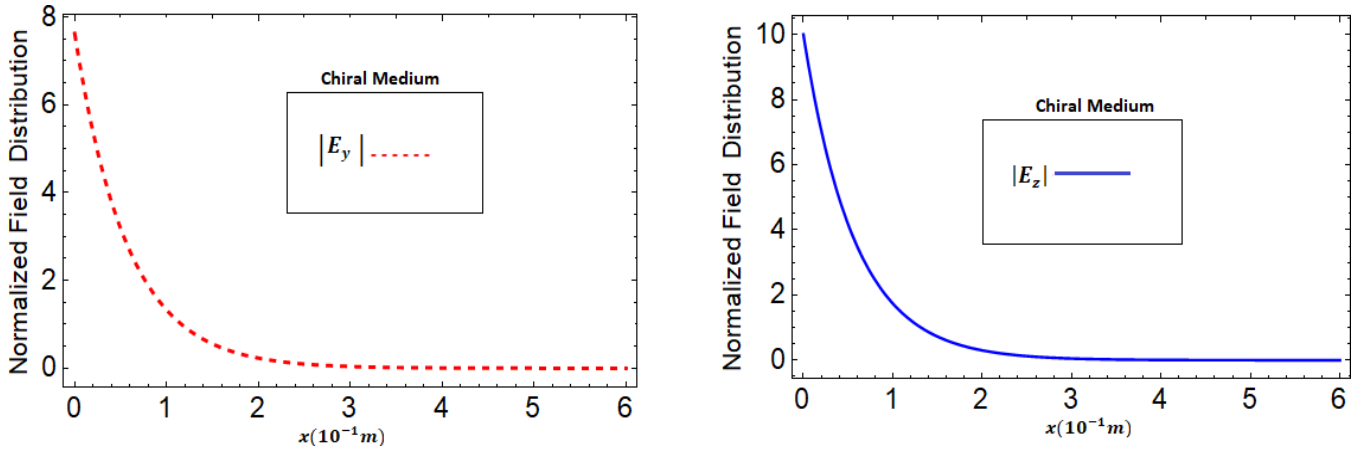

Figure 5: Field profiles for chiral medium.

Conclusion

A theoretical framework for comprehending the hybrid EMSW interaction at the chiral– magnetized plasma interface has been investigated. To understand the confinement of EMSWs for the proposed design, the influence of the magnetized plasma parameters such as the plasma frequency ω_p, the cyclotron frequency ω_c, and chirality of chiral material with respect to operating surface wave frequency in the THz range are explored. It has been observed that the effective mode index of the proposed design is very sensitive to plasma parameters. Furthermore, the chirality parameter may be used to control and adjust the effective mode index of EMSWs, which is a key factor in the confinement of EMSWs. These findings reveal that chiral and magnetized plasma have distinct properties that may significantly influence wave propagation and confinement, therefore may be

useful in improving performance of advanced applications like signal processing and chiral sensing. To verify the surface wave conditions, the field profiles for E_y and E_z of the chiral material were also presented. These results highlight how versatile EMSWs are in engineering and open the new avenue in the development of tunable photonic and communication technologies.

Acknowledgments: The authors would like to thank the Higher Education Commission of Pakistan for the funding through HEC Indigenous Ph.D. Fellowship Program.

Disclosures: The authors have no conflicts of interest to declare.
Data availability: Data underlying the results presented in this paper are not publicly available at this time but may be obtained from the authors upon reasonable request.

References

1. Gogoi, N. and P.P. Sahu, All-optical tunable power splitter based on a surface plasmonic two-mode interference waveguide. Applied optics, 2018. 57(10): p. 2715- 2719.
2. Gogoi, N. and P.P. Sahu, All-optical surface plasmonic universal logic gate devices. Plasmonics, 2016. **11**(6): p. 1537-1542.
3. Montazeri, M. and A. Abdoli-Arani, Energy and trajectory of injected electron in the mixed circular and elliptical waveguide filled magnetized plasma. Optik, 2021. **225**: p. 165349.
4. Datsko, V.N. and A.A. Kopylov, On surface electromagnetic waves. 2008, UFN.
5. Arif, M., et al., Propagation properties of plasma-filled parallel plate waveguide (PPWG) surrounded by black phosphorus (BP) layers. Waves in Random and Complex Media, 2024: p. 1-11.
6. Serrera, G., et al., Enhanced optical chirality with directional emission of Surface Plasmon Polaritons for chiral sensing applications. Journal of Quantitative Spectroscopy and Radiative Transfer, 2022. **284**: p. 108166.
7. Bassiri, S., C. Papas, and N. Engheta, Electromagnetic wave propagation through a dielectric–chiral interface and through a chiral slab. JOSA A, 1988. **5**(9): p. 1450- 1459.
8. Flood, K.M. and D.L. Jaggard, Single-mode operation in symmetric planar waveguides using isotropic chiral media. Optics letters, 1996. **21**(7): p. 474-476.
9. Silverman, M. and R. Sohn, Effects of circular birefringence on light propagation and reflection. American Journal of Physics, 1986. **54**(1): p. 69-76.
10. Engheta, N. and P. Pelet, Surface waves in chiral layers. Optics letters, 1991. **16**(10): p. 723-725.
11. ARIF, M., et al., Characteristics of metal–uniaxial chiral–metal plasmonic waveguide structure. Optoelectronics and Advanced Materials-Rapid Communications, 2024. **18**(July-August 2024): p. 313-318.
12. Arif, M., et al., Dispersion Properties in Uniaxial Chiral–Graphene–Uniaxial Chiral Plasmonic Waveguides. Plasmonics, 2024: p. 1-10.
13. Arif, M., et al., Excitation of Surface Plasmon Polaritons (SPPs) at Uniaxial Chiral- Graphene Planar Structure. Plasmonics, 2024: p. 1-9.
14. Gric, T. and E. Rafailov, Absorption enhancement in hyperbolic metamaterials by means of magnetic plasma. Applied Sciences, 2021. **11**(11): p. 4720.
15. Qi, L., D. Sun, and S.M.A. Shah, Tunable surface plasmon polaritons in magnetized collision plasma and dielectric. Applied Physics Express, 2019. **12**(6): p. 062004.
16. Abrahimi, B., A. Abdoli-Arani, and Z. Rahmani, Electromagnetic Fields and Trajectory of Injected Electron Inside an Elliptical Coaxial Magnetized Plasma Waveguide. IEEE Transactions on Plasma Science, 2020.
17. Girka, I.O., I.V. Pavlenko, and M. Thumm, Electromagnetic energy rotation along plasma-metal interface in cylindrical waveguides initiated by azimuthal surface waves. Physics of Plasmas, 2019. **26**(2): p. 022113.
18. Girka, I.O., I.V. Pavlenko, and M. Thumm, Electromagnetic energy rotation by azimuthal surface waves along plasma-metal interface around a cylindrical metallic rod placed into infinite magnetized plasma. Physics of Plasmas, 2019. **26**(5): p. 052103.
19. Li, R., et al., Hybridized surface plasmon polaritons at an interface between a metal and a uniaxial crystal. Applied Physics Letters, 2008. **92**(14): p. 141115.
20. Laroussi, M. and J.R. Roth, Numerical calculation of the reflection, absorption, and transmission of microwaves by a nonuniform plasma slab. IEEE Transactions on Plasma Science, 1993. **21**(4): p. 366-372.
21. Petrin, A.B., On the transmission of microwaves through plasma layer. IEEE transactions on plasma science, 2000. **28**(3): p. 1000-1008.
22. Bevc, V. and T.E. EVERHAR, Fast-wave propagation in plasma-filled waveguides. INTERNATIONAL JOURNAL OF ELECTRONICS, 1962. **13**(3): p. 185-212.
23. Ivanov, S. and E. Alexov, Electromagnetic waves in a plasma waveguide. Journal of plasma Physics, 1990. **43**(1): p. 51-67.
24. Shen, H.M., Plasma waveguide: A concept to transfer electromagnetic energy in space. Journal of applied physics, 1991. **69**(10): p. 6827-6835.
25. Shen, H.M. and H.Y. Pao, The plasma waveguide with a finite thickness of cladding.

Journal of applied physics, 1991. **70**(11): p. 6653-6662.

26. Majedi, S., S. Khorashadizadeh, and A. Niknam, Propagation of surface waves in a spin 1/2 magnetized collisional quantum plasma half-space. The European Physical Journal Plus, 2018. **133**: p. 1-7.

27. Zhu, S., B. Wang, and B. Guo, Dispersion relation of graphene surface plasmon by using a quantum hydrodynamic model. Superlattices and Microstructures, 2020. **142**: p. 106516.

28. Zhang, Q., et al., Dispersion, propagation, and transverse spin of surface plasmon polaritons in a metal-chiral-metal waveguide. Applied Physics Letters, 2017. **110**(16): p. 161114.

29. Umair, M., et al., Dispersion characteristics of hybrid surface waves at chiral-plasma interface. Journal of Electromagnetic Waves and Applications, 2020: p. 1-13.